Local Dynamics of Poly(ethylene oxide) in Solution. 2. Vector Autocorrelation Functions and Motional Anisotropy

Michael M. Fuson* and Kent H. Hanser

Department of Chemistry and Biochemistry, Denison University, Granville, Ohio 43023

M. D. Ediger

Department of Chemistry, University of Wisconsin, 1101 University Avenue, Madison, Wisconsin 53706

Received January 14, 1997; Revised Manuscript Received July 18, 1997[⊗]

ABSTRACT: The anisotropy of the local dynamics of poly(ethylene oxide) in toluene solution has been characterized using molecular dynamics simulations and NMR coupled spin relaxation experiments. Ratios of second rank correlation times calculated from the trajectories, such as that between correlation times describing the reorientation of vectors parallel (τ_z) and perpendicular ($\tau_\perp$) to the local chain axis, reproduce all trends seen in values obtained from NMR coupled spin relaxation experiments. The magnitude of the anisotropy is larger than that observed for PEO in aqueous solution but smaller than that of polyethylene in biphenyl solution. Correlation function shapes are markedly nonexponential, in contrast to those seen for recent simulations of polyisoprene in solution but similar to those seen for n-$C_{44}H_{90}$ melts. Comparison of correlation functions calculated from regions of the trajectory near and between conformational transitions indicates that transitions have a role in producing larger anisotropies and more nonexponential correlation functions. Decay in correlation functions in the absence of conformational transitions supports the suggestion that coupled small amplitude motions of groups of torsions (coupled librations) can be an important relaxation mechanism.

I. Introduction

In this paper we report a study of the local dynamics of poly(ethylene oxide) (PEO) in dilute toluene solution using both molecular dynamics simulations and NMR-coupled spin relaxation experiments. Using the molecular dynamics simulations reported in the previous paper,[1] we calculate vector autocorrelation functions, both in order to understand the mechanisms leading to loss of orientational order and as a way to characterize the anisotropy in the local dynamics. The anisotropy is then compared to results obtained from NMR coupled spin relaxation experiments. This represents the first time these techniques have been applied in tandem to a polymer system.

The local dynamics of a polymer chain are largely influenced by torsional motions, such as librations and conformational transitions, which affect fairly small regions of a polymer chain. In the previous paper[1] we showed that for PEO in toluene solution at 338 K conformational transitions are very frequent, for a given bond less than 10 ps apart on average. The motion accompanying a conformational transition is localized to about 8−10 atoms on either side of the transition. The mechanism of localization of the motion involves torsional adjustments in several neighboring bonds, sometimes resulting in a second correlated conformational transition.

Experimental investigations of local dynamics in polymer systems often involve measurement of "correlation times" by dielectric relaxation or NMR spin relaxation. For example, the correlation time obtained from an NMR ^{13}C T_1 relaxation time is the time integral of the P_2 autocorrelation function of a unit vector pointing in the direction of the CH bond:

$$\tau_c = \int_0^\infty \frac{1}{2}\langle 3(e_{CH}(0)\cdot e_{CH}(t))^2 - 1\rangle \, dt \qquad (1)$$

The anisotropy of the local dynamics can be characterized by examining correlation times associated with unit vectors related to the local symmetry of the polymer chain. These are illustrated in Figure 1. The z axis is parallel to the local chain axis and is often called the chord vector (from the chord between C_{n-1} and C_{n+1}). The x axis, or bisector, bisects the CCC angle or, equivalently, the HCH angle. The y axis, or out-of-plane vector, is perpendicular to x and z and is parallel to the HH vector. Recent computer simulations of polyethylene dynamics show that the correlation time for z axis reorientation is significantly longer than the other two.[2−5] In contrast, polyisoprene dynamics are nearly isotropic.[6,7]

Spin relaxation studies that take advantage of the multiple interactions among several scalar coupled spins, for example, $^{13}CH_2$, can measure all three of these correlation times.[8,9] For a methylene or methyl group with two or three identical CH interactions, the common practice has been to regard them as independent, and the resulting ^{13}C relaxation rate, $1/T_1$, then scales with the number of attached hydrogens. However, for three or more spins a complete description of the relaxation also includes cross-correlation terms between pairs of dipolar vectors, such as the two different CH vectors in a methylene group.[10−12] The traditional approach has been to regard these as either small or unimportant. Additionally, if the ^1H spins are decoupled to enhance ^{13}C sensitivity, the ^{13}C spin will almost always relax with an "effective" single exponential recovery law as the multiple exponential relaxation behavior of the coupled spins is obscured with the collapse of the proton-induced multiplet under decoupling.[13] Study of the fully coupled multiplets provides significant additional information. For a methylene group, four independent spectral densities are required to describe the relaxation

[⊗] Abstract published in *Advance ACS Abstracts,* September 1, 1997.

S0024-9297(97)00035-1 CCC: $14.00

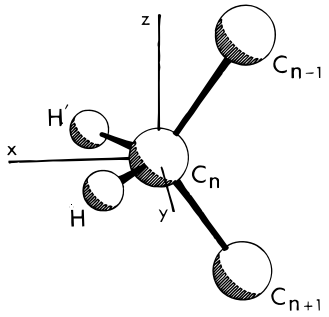

Figure 1. Orientation of the Cartesian axis system in the molecular frame.

even in the extreme narrowing limit. These can be used to calculate the three correlation times described above, plus a fourth one describing the reorientation of something looking like a d_{xy} orbital.[8]

Coupled spin relaxation methods have been used to study local dynamics in a series of polyethers and polyethylene (PE) in solution (note that PE can be viewed as a polyether, $(-O-(CH_2)_m-)$, with $m = \infty$).[14−16] A wide range of behaviors has been observed, with poly(oxymethylene) being the most isotropic, PEO and poly(tetramethylene oxide) intermediate cases, and PE the most anisotropic. Although the degree of anisotropy observed in simulations of PE melts is roughly comparable to that obtained from the NMR experiments on PE solutions, the molecular origin of these anisotropies is not clear. The present study is the first of several that have been undertaken in an attempt to understand the connection between chain structure, with its associated torsional potentials, and the anisotropy of the local dynamics.

PEO in toluene has been chosen for study for several reasons. PEO is a technologically and biomedically important polymer. While NMR coupled spin relaxation data have been obtained for PEO in D_2O solution,[15] toluene was selected as the solvent for the present study both to avoid troubling issues with respect to modeling strongly associated liquids and to allow direct comparison to previous simulations of polyisoprene (PI) solutions.[6] Some recent molecular dynamics simulations of PEO in solution[17−20] and in the melt[21−23] have appeared, but they have focused primarily on structural issues. While Tasaki has briefly examined the local dynamics of a 15mer of PEO in benzene,[20] most of the previous simulations of polymers that focus on local dynamics have been done on hydrocarbons[2−5,24−26] and so examining a heteroatom polymer allows us to broaden the range of systems considered.

II. Simulation Description

The molecular dynamics simulations analyzed here were generated using *Discover 2.9.5* (Biosym Technologies, San Diego, CA) on a Silicon Graphics Power Challenge 4 workstation. A 54mer of PEO (2397 MW, 163 backbone atoms) was surrounded by 207 toluenes to give a system that is 11.2% by weight polymer. All atoms of both the polymer and the solvent were explicitly represented to give a total of 3486 atoms. The simulations were run with periodic boundary conditions at a constant temperature of 338 K and a constant pressure of 1 bar using an 8 Å cutoff for nonbonded interactions. One femtosecond time steps were used in the calculation, but the atomic coordinates were saved only every 100 fs. Each of four starting configurations was run for a total of 1200 ps, with the final 990 ps of each run used for analysis. Further details are given in the previous paper.[1]

III. NMR Experiments and Results

Experimental Methods. Poly(ethylene oxide) (MW = 20 000; $M_w/M_n = 1.13$) was obtained from Polysciences (Warrington, PA). Deuterated toluene (99.6% D) was obtained from Cambridge Isotope Laboratories (Woburn, MA). Both materials were used without further purification. The sample was made by dissolving 0.025 g of PEO in 2.50 g of toluene. The sample was subjected to five freeze−pump−thaw cycles and sealed under vacuum in a 10 mm NMR tube.

Spectra were acquired on a Bruker AC300 NMR spectrometer operating at a ^{13}C frequency of 75.5 MHz. The temperature for all runs was 330 ± 1 K. Spectral widths were 2000 Hz for all experiments. For each spectrum, 480 scans of 4096 data points were acquired. FID's were baseline corrected, then zerofilled to 16 384 data points. Six hertz of line broadening was applied before Fourier transformation.

Spin relaxation measurements were made after four different perturbations of the coupled $^{13}CH_2$ spin system. These were (1) a ^{13}C 180° pulse inverting the ^{13}C triplet, (2) a ^1H 180° pulse inverting the ^1H doublet, (3) a low-power ^1H pulse inverting only the upfield line of the ^1H doublet,[27] and (4) a J pulse preparation on the ^1H magnetization that inverts the outer lines of the ^{13}C triplet.[28] In each experiment the initial perturbation was followed by a variable delay and a 90° ^{13}C sampling pulse. Eighteen delay times were used for each experiment, ranging from 0.0031 to 30 s. Delays were randomly ordered to reduce systematic errors. The longest delay was at least 10 times the nominal T_1 of the sample. Peak amplitudes of the ^{13}C triplet were obtained after application of a linear baseline correction over a 500 Hz region centered on the ^{13}C multiplet.

Data Fitting Procedures. Instead of characterizing the behavior of individual resonance lines, it is convenient to analyze the data in terms of "magnetization modes" that are linear combinations of line intensities.[9,10,12] Three magnetization modes of the $^{13}CH_2$ spin system can be obtained from observation of the ^{13}C multiplet: (1) ${}^a\nu_C$, the total ^{13}C magnetization; (2) ${}^a\nu_{+-+}$, the difference between the inner and outer line intensities of the ^{13}C triplet; (3) ${}^s\nu_{+0-}$, the difference between the intensities of the two outer lines of the ^{13}C triplet.

The time evolution of the magnetization modes is governed by a Redfield-type relaxation matrix whose elements are combinations of spectral densities arising from all relaxation mechanisms active in the sample.[9,10,12] For this study, spectral densities included in the fit include four frequency independent spectral densities describing the dipolar relaxation of a methylene group ($^{13}CH_2$) in the limit of extreme narrowing (J_{CHCH}, $J_{HH'HH'}$, $J_{CHCH'}$, and $J_{CHHH'}$ where pairs of subscripts specify a dipolar interaction). Random field spectral densities are also included to account for other relaxation mechanisms operating in the sample, primarily remote dipolar interactions. For the methylene spin system, a complete set of random field spectral densities would include an autocorrelation term at the carbon (j_C), an autocorrelation term at each hydrogen (j_H), and a cross-correlation term between the two hydrogens ($j_{HH'}$). At high fields or in a more anisotropic electronic environment caused by insertion of a heteroatom into the polymer chain, cross-correlation between chemical shift anisotropy (CSA) and dipolar relaxation mechanisms can be significant.[29,30] Where appropriate, this requires inclusion of four more spectral densities in the fit. In the current study the only one of these terms that is significantly different from zero is $J_{CH,C}$, which expresses the cross-correlation between the CH dipolar interaction and the carbon CSA tensor. The other three terms are set to zero in the final fits reported here.

Rigorous characterization of longer range dipolar interactions as random fields requires that both the rotational and translational motion of the interacting spins be independent.[31,32] This independence of motion is not satisfied for protons bonded to carbons adjacent to the methylene group of interest. A study of isotopomers of [5-^{13}C]nonane has shown that inclusion of random field terms in the relaxation matrix

Table 1. Poly(ethylene oxide) Spectral Densities (s^{-1})

J_{CHCH}	0.051(1)	$j_{HH'}$	0.5(4)
$J_{HH'HH'}$	0.037(5)	$J_{CH,C}$	−0.028(1)
$J_{CHCH'}$	0.017(3)	$J_{CH,H'}$	[0]
$J_{CHHH'}$	0.032(1)	$K_{CH,H'}$	[0]
j_C	[0][a]	$J_{HH,H}$	[0]
j_H	0.05(8)		

[a] Square brackets indicate values that were fixed during the fit.

Table 2. Correlation Times and Anisotropies from NMR (ps)

$\tau_\perp = 6.7(13)$	$\tau_z/\tau_\perp = 3.7(8)$
$\tau_z = 23.1(17)$	$\tau_z/\tau_{xy} = 5.4(7)$
$\tau_{xy} = 4.3(4)$	$\tau_\perp/\tau_{xy} = 1.5(3)$

is not enough to allow accurate measurement of all four dipolar spectral densities in the presence of protons on neighboring carbons. However, that study showed that as long as the random field term j_C is held equal to zero in the fitting procedure, then J_{CHCH}, $J_{CHCH'}$, and $J_{CHHH'}$ may be reliably evaluated. $J_{HH'HH'}$ remains strongly correlated to j_H.[33] The results reported here conform to this practice.

Data were analyzed using a multiparameter fitting routine, as described previously.[33] In addition to spectral densities, variables included pulse efficiencies, equilibrium intensities, and scaling factors compensating for line width differences and instrumental artifacts.

Results. Final fitted values of the spectral densities are reported in Table 1. The uncertainties in the last digit (given in parentheses) reported here and in other tables are standard errors or 68% confidence intervals. As discussed above, $J_{HH'HH'}$ and j_H are highly correlated and the errors reported here do not fully represent their uncertainty, even given the high uncertainty reported for j_H. Absolute uncertainties for J_{CHCH}, $J_{CHCH'}$, and $J_{CHHH'}$ are small, although the small magnitude of $J_{CHCH'}$ means that the relative uncertainty is substantial, 18%.

The three dipolar spectral densities that have been reliably evaluated can be reexpressed in terms of three second rank autocorrelation times ($\tau_\perp = \tau_x = \tau_y$, τ_z, and τ_{xy}). The transformation to Cartesian correlation times requires that the geometry of the spin system be known.[8] For the CH bond length we shall adopt the value of 1.11 Å obtained in the electron diffraction study of the small-molecule analog of PEO, 1,2-dimethoxyethane.[34] The HCH angle was not determined in that study; therefore we shall adopt the value of 108.5° from electron diffraction studies of small alkanes.[35] The Cartesian correlation times calculated using these parameters and their ratios (the anisotropies) are given in Table 2. Detailed discussion of the experimentally determined anisotropies is given below, in comparison to the MD simulation results.

Compared to previous coupled spin relaxation measurements of PEO in D_2O at 298 K,[15] the correlation times reported here are shorter by factors ranging from 4−10, with larger anisotropies reported in the present study. These changes could reflect differences in the local dynamics due to temperature and solvent. There is substantial evidence that PEO adopts different conformations in polar and nonpolar solvents.[36] Further investigation of the solvent dependence of PEO local dynamics is underway.

In the following section we will compare the results reported here to those calculated from molecular dynamics simulations. The two sets of results come from PEO's of differing molecular weights (20 000 vs 2400) and solutions of differing concentrations (1% vs 11%). Previous studies suggest that these differences should not lead to important changes in the local dynamics. Extensive NMR spin relaxation studies of aqueous solutions of PEO show that ^1H, ^2H, and ^{13}C T_1 and T_2 relaxation times are independent of molecular weight above about 1300 (corresponding to a degree of polymerization of 30) and of concentration up to 10% by weight polymer.[37−39] ^{13}C T_1's of PEO in C_6D_6 are within experimental error (10%) of each other for 5 and 10% by weight solutions.[40] Thus, the differences between the NMR spin relaxation measurements and the molecular dynamics simulations should not prevent meaningful comparison of their results.

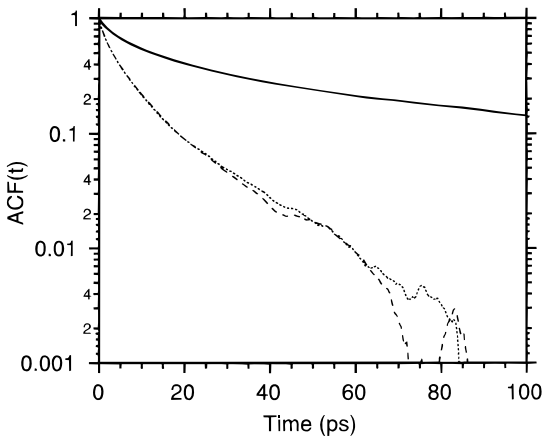

Figure 2. Semilog plot of P_1 autocorrelation functions for Cartesian functions: (···) x; (- - -) y; (—) z.

IV. Vector Autocorrelation Functions and the Anisotropy of Local Dynamics

We have seen that coupled spin relaxation experiments allow determination of three (or four) second-rank correlation times describing the reorientation of a given methylene unit in a flexible polymer chain. The ratios of these correlation times characterize the anisotropy of the local motion.

These same quantities can be calculated from the simulated trajectories. Correlation times describing the reorientation of unit vectors aligned with the x, y, or z axes as defined in Figure 1 can be calculated from the time integrals of their P_2 autocorrelation functions as in eq 1. τ_{xy} is given by the time integral of

$$\mathrm{ACF}_{xy}(t) = \left\langle \frac{(e_x(0)\cdot e_x(t))(e_y(0)\cdot e_y(t)) + (e_x(0)\cdot e_y(t))(e_y(0)\cdot e_x(t))}{2} \right\rangle \quad (2)$$

where e_x is a unit vector pointing in the x direction. Similarly, P_1 correlation times can also be calculated for unit vectors lying along x, y, or z using

$$\tau_i = \int_0^\infty \langle e_i(0)\cdot e_i(t)\rangle \, \mathrm{d}t \quad (3)$$

P_1 and P_2 autocorrelation functions calculated from the simulations are given in Figures 2 and 3, respectively. For both P_1 and P_2 functions, the z vector correlation decays most slowly. The x and y functions decay more quickly and are nearly identical. The xy P_2 function decays most rapidly, as it is sensitive to reorientation about all three axes.

For these and all subsequent calculations, data from the five repeat units on either end of the PEO chain have been omitted to minimize end effects. It has been estimated from NMR data that the final three repeat units at the ends of the chains have dynamic properties that are perturbed by the chain end.[39]

Shapes of Autocorrelation Functions. As seen from the nonlinearity of the semilog plots in Figures 2 and 3, all of the correlation functions are nonexponential. To quantify the extent of the nonexponentiality, these functions were fit to a Kohlrausch−Williams−Watts (KWW) function[41]

$$\mathrm{ACF}(t) = \mathrm{e}^{-(t/\tau)^\beta} \quad (4)$$

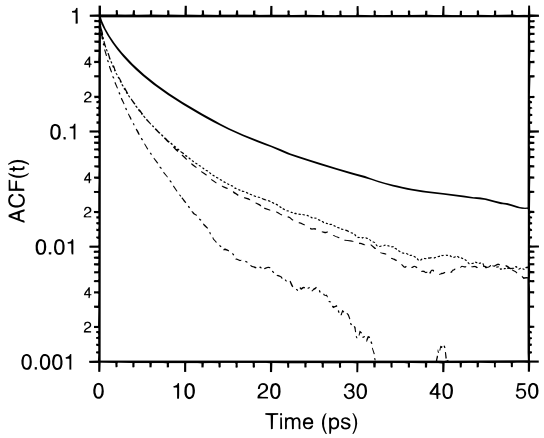

Figure 3. Semilog plot of P_2 autocorrelation functions for Cartesian functions: (···) *x*; (- - -) *y*; (—) *z*; (— · —) *xy*.

Table 3. KWW Parameters for Vector ACFs

	P_1		P_2	
	τ_{KWW} (ps)	β	τ_{KWW} (ps)	β
τ_x	5.39(1)	0.66(1)	1.55(1)	0.54(1)
τ_y	5.33(1)	0.67(1)	1.60(1)	0.56(1)
τ_z	26.8(1)	0.50(1)	4.06(1)	0.59(1)
τ_{xy}			1.14(1)	0.61(1)

The farther β deviates from unity, the more nonexponential the function. Results of these fits are given in Table 3. The fits obtained are excellent, with the root mean square deviation of the data from the fitted line less than 1.3% of full scale in all cases.

The shapes of the P_2 autocorrelation functions and the KWW β's found here are similar to that found for the CH P_2 autocorrelation function for the methylenes at the center of a PEO 15mer in benzene.[20] Furthermore, the correlation functions obtained here are similar in shape to those obtained previously for a *n*-$C_{44}H_{90}$ melt,[5] except for the absence of a long time tail. In that study the correlation functions were fit to a KWW function that had been modified by adding an additional exponential term. The β values obtained for the P_1 correlation functions in the two simulations agree almost exactly, while the P_2 β values obtained here are about 0.1 larger than in the C_{44} melt at 400 K. In contrast, a simulation of polyisoprene in toluene solution produced correlation functions that showed a rapid initial drop followed by nearly exponential decays.[6] Simulations of polyisoprene[7] and *cis*-polybutadiene[26] melts gave somewhat intermediate results: still two well-separated time scales, but with a rapid initial decay followed by a nonexponential decay.[7] The rapid initial decays in these simulations have been attributed to librational motion. Average conformational transition times for PI in solution and in the melt were much longer than for either PEO or C_{44}, allowing observation of two separate time scales in the former cases. Possible roles of conformational transitions in determining the shape of the correlation functions will be examined below.

Anisotropy of Local Dynamics. To examine the anisotropy of the local dynamics more explicitly, it is useful to obtain correlation times for the reorientation of the various vectors and examine their ratios. This also allows direct comparison to the NMR coupled spin relaxation results. All of the correlation functions shown in Figures 2 and 3 decay to zero within 400 ps. Therefore, we have calculated correlation times by numerical integration over this interval. The correlation times and their ratios are given in Table 4. Also given in Table 4 for comparison purposes are the NMR results.

Table 4. Vector Correlation Times (ps) and Anisotropies

	τ_x	τ_y	τ_z	τ_{xy}	$\tau_z/\tau_\perp$	τ_z/τ_{xy}	$\tau_\perp/\tau_{xy}$
P_1	7.2(2)	7.0(1)	47(4)		6.6(6)		
P_2	3.4(3)	3.0(2)	7.7(7)	1.7(1)	2.4(3)	4.5(5)	1.8(2)
NMR[a]	6.3(13)		23(2)	4.3(4)	3.7(8)	5.4(7)	1.5(3)

[a] Values from Table 2.

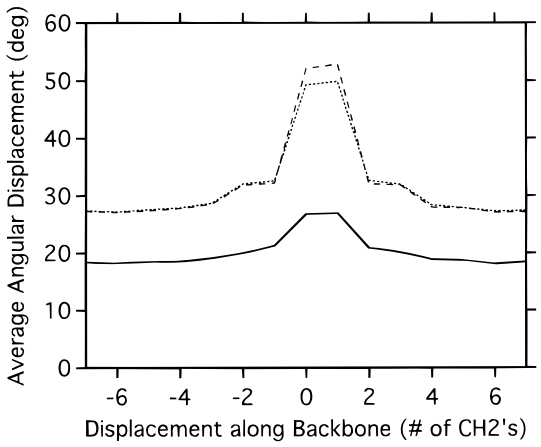

Figure 4. Average angular displacement of Cartesian axes associated with CC conformational transitions: (···) *x*; (- - -) *y*; (—) *z*.

Examination of the P_2 correlation times in Table 4 shows that they reproduce the trends in the NMR data accurately while agreeing in absolute magnitude within a factor of 2 or 3. This level of absolute agreement is understandable in light of the somewhat low density and the slight mismatch in temperatures between experiment and simulation. Preliminary results from a simulation of poly(tetramethylene oxide) in toluene solution that yields a more realistic density again reproduce all the trends in the NMR data and show even better absolute agreement of the time scales.[42] We are confident that the simulations are sufficiently accurate that close examination of the local dynamics will shed light on the origin of the experimentally observed anisotropies.

Role of Conformational Transitions. In comparison to other polymer systems recently simulated, the local dynamics of PEO are intermediate in their anisotropy. C_{44} melts show a ratio of $\tau_z/\tau_\perp$ of 9.3, while the same ratio for polyisoprene either in the melt or in solution is 1.7. One possible explanation for the range of anisotropies exhibited is that conformational transitions contribute in different ways to correlation function decay in these systems. To examine this further for PEO in solution, we calculate the average angle between the direction of the *x*, *y*, and *z* axes before and after a transition for methylenes in the neighborhood of a conformational transition:

$$\langle \arccos(e_i(\tau_{trans}-\Delta t)\cdot e_i(\tau_{trans}+\Delta t))\rangle_j \qquad (5)$$

where $i = x$, y, or z, τ_{trans} is the transition time (defined as the time at which a torsion crosses over a barrier, in the process of continuing to the bottom of the adjacent potential well), and j labels the position of the methylene relative to the conformational transition and is defined to be 0 and 1 for methylenes immediately adjacent to the transition. Figure 4 shows the results of such a calculation for conformational transitions centered at

a CC torsion with a Δt of 0.2 ps. Various choices of Δt from 0.1 to 2.0 ps change the magnitude of the effect, but not the pattern observed. The local variations caused by conformational transitions have disappeared for Δt's as large as 5.0 ps.

The average angular displacement of *x* and *y* vectors is very similar. They reorient by larger angles than *z* vectors both in the section of the chain immediately adjacent to the transition and further away. Far away from the transition, *x* and *y* reorient by 27° and *z* by 18°, on average. This is enough to cause a P_2 correlation function to decay by 30% and 15%, respectively, during this time interval. A conformational transition perturbs *x* and *y* strongly, leading to an average angular change of about 50°, enough to reduce a P_2 correlation function by 90%. The *z* axis, on the other hand, is perturbed more weakly, increasing its average range of motion to be similar to that of the *x* and *y* axes in the absence of conformational transitions. Thus, conformational transitions are strongly implicated in anisotropic dynamics.

Another way to illustrate the impact of conformational transitions on the anisotropy of the local dynamics is to divide the simulated trajectories into sections (1) *near* conformational transitions and (2) *between* conformational transitions and to calculate the P_2 correlation functions for both regions separately. We define these regions by mapping out blocks extending four methylenes to either side of a transition and extending from 0.5 ps before a transition to 0.5 ps afterward. This is the same definition used in the previous paper when coupled librations were examined in the absence of conformational transitions.[1] Correlation functions for the regions between transitions have been calculated previously for PI melt, solution, and vacuum simulations.[6,7,43] In the present case, there are enough transitions in the trajectories that the blocks mapped out around them are frequently overlapping, enough so to allow calculation of the first 10 ps or so of a correlation function solely within the blocks. Figure 5 shows semilog plots of the PEO P_2 correlation functions calculated both near and between transitions.

The behaviors of the functions in these two regions are dramatically different from each other and from those calculated for the full trajectory (Figure 3). Near the conformational transitions, the functions are more nonexponential, decrease more rapidly, and vary more widely in rates of decrease (i.e., the dynamics are more anisotropic). Between the transitions, the functions become nearly exponential after the first 2 ps, decrease more slowly, and decrease at more similar rates. To characterize these differences, we have summarized in Table 5 1/*e* relaxation times and their ratios for the P_2 correlation functions near the transitions, between the transitions, and for the full trajectories. We tabulate 1/*e* relaxation times instead of correlation times because we are unable to calculate the correlation functions for sufficiently long times in the sectioned trajectories. As expected, Table 5 shows that the relaxation times and anisotropies for the regions of the trajectories near conformational transitions and between conformational transitions bracket those of the full trajectory. Regions near conformational transitions show shorter relaxation times and higher anisotropies.

Mechanisms of Correlation Function Decay. In a recent paper, Moe and Ediger have assessed the relative contributions of librations, conformational transitions, and some additional mechanism, probably coupled librations (cumulative motion of groups of

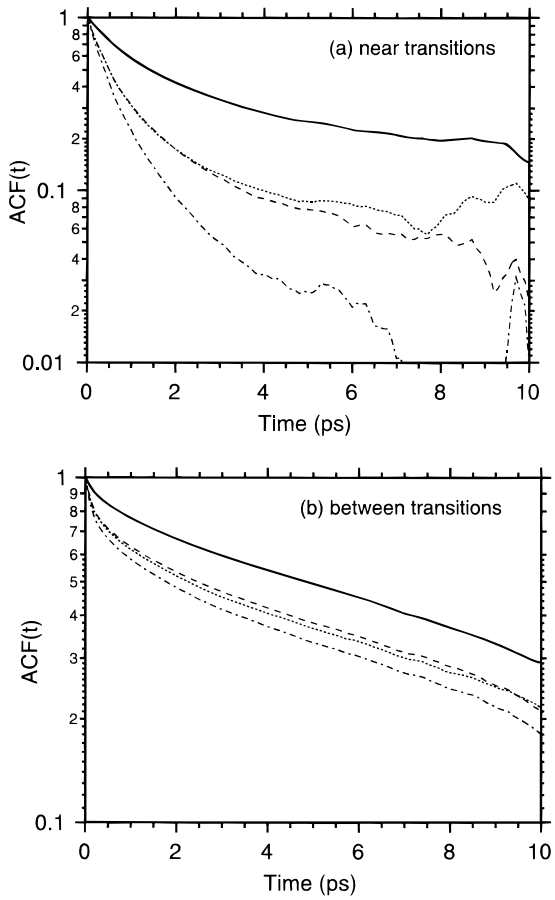

Figure 5. Semilog plots of P_2 autocorrelation functions for Cartesian functions (a) near conformational transitions and (b) between conformational transitions: (···) *x*; (- - -) *y*; (—) *z*; (•—•) *xy*.

Table 5. 1/*e* Relaxation Times (ps) and Their Ratios

	τ_x	τ_y	τ_z	τ_{xy}	$\tau_z/\tau_\perp$	τ_z/τ_{xy}	$\tau_\perp/\tau_{xy}$
near transitions	0.78	0.79	2.6	0.58	3.3	4.5	1.4
full trajectory	1.6	1.6	4.0	1.2	2.5	3.4	1.4
between transitions	5.0	5.4	8.0	4.1	1.5	2.0	1.3

torsions), to P_2 correlation function decay in simulations of polyisoprene.[43] We perform a similar assessment here. Although the rapid decay in the correlation functions due to librations is difficult to isolate in the full correlation functions for PEO in solution (Figure 3), it is clearly revealed in the correlation functions calculated in sections between trajectories (Figure 5b). Extrapolating the linear regions back to the origin, we can estimate that about 20% of the *z* vector autocorrelation function decays due to libration, 35% of the *x* and *y* functions, and 42% of the *xy* function. These proportions compare to 10%, 25%, and 35%, respectively, for polyisoprene in solution. The differences between the two polymers are likely due to the broader range of changes in torsion angles seen at short times in POE than in polyisoprene (as shown in Figure 2 of the previous paper[1] versus Figure 5 of ref 6).

The relative importance of conformational transitions and alternative mechanisms of correlation function decay, such as coupled librations for the remaining decay of the correlation functions, can be estimated by taking the relaxation rates, with and without conformational transitions, as proportional to the inverse of the 1/*e* relaxation times given in Table 5. Doing so, we estimate that conformational transitions are about twice

as important as alternative mechanisms for correlation decay for *x* and *y* functions and equally important for the *z* function. Both mechanisms were estimated to be about equally important to all of these functions for polyisoprene in solution, while conformational transitions were estimated to be 2−3 times more important in the melt.[43] The differences between the behavior of the two polymers in solution may be related to the very different average conformational transition times. For PEO, average conformational transition times were less than 10 ps, while for polyisoprene in solution, they average 122 ps. For polyisoprene in the melt, conformational transition times are still much longer than for PEO (averaging 81 ps), but alternate relaxation mechanisms such as coupled libration seem to be much less efficient processes for vector reorientation than in solution.

V. Concluding Remarks

In this paper we have characterized the anisotropy of the local dynamics of poly(ethylene oxide) in toluene solution, both by NMR coupled spin relaxation and by molecular dynamics simulation. Experimental measurements of second rank correlation times for reorientation of functions aligned with a Cartesian axis system in the molecular frame of reference show that the *z* axis (the local chord axis) reorients significantly slower than either the *x* or *y* axes (also known as the bisector and out-of-plane axes). The anisotropy is larger than previously observed for PEO in D_2O at 298 K but is consistent with observations for other linear polymers. Molecular dynamics simulations yield correlation times that are smaller in absolute magnitude by a factor of 2 or 3 but that correctly reproduce all the trends in the experimental data.

Differences in the vector autocorrelation functions calculated in regions of the trajectory near conformational transitions and between conformational transitions clearly indicate that conformational transitions play a major role in determining both the shape of the correlation functions and the magnitude of the anisotropy of the local dynamics. However, differences in these properties for PEO, PI, and C_{44} also show that it is difficult to specify the exact nature of that role. There are several possible origins for these differences, including (1) the fraction of correlation function decay caused by conformational transitions, (2) the extent of chain (or vector) reorientation at a conformational transition, and (3) the impact of correlated conformational transitions. These three possibilities are discussed in the next three paragraphs.

Earlier we estimated that conformational transitions were about twice as important as other mechanisms for correlation function decay for PEO in solution and PI melts and equally important for PI in solution. This does not seem to correlate with the magnitude of the anisotropy in these systems, where both PI systems have similar anisotropies, which are small compared to that of PEO. It does correlate reasonably well with the nonexponentiality of the correlation functions.

The extent of vector reorientation associated with a conformational transition can vary substantially between polymers. Here we have seen that the average angular displacement of the *x* and *y* axes (perpendicular to the *z* or chord axis) nearly doubles from 27° to 50° for methylenes at the end of a bond undergoing a conformational transition. For polyisoprene a similar calculation shows that CH vectors, which lie in the *xy* plane, undergo displacements that vary by a factor of 2 depending on the type of bond undergoing a conformational transition but that are similar in solution and melt simulations (see Figure 8 of ref 41). The similarity of the anisotropy of the local dynamics of polyisoprene solutions and melts, despite differences in the relative importance of conformational transitions to correlation function decay and in shapes of the correlation functions, suggests that this may be an important determinant of the anisotropy. The relation of the magnitude of average angular displacement to other structural or dynamic characteristics of the polymer remains to be determined.

Recent simulations of polymer dynamics have paid considerable attention to the role of a second "correlated" or "cooperative" conformational transition in localizing the chain motion caused by conformational transitions. These are often analyzed in terms of "first failure pairs" occurring at second neighbor torsions. Analysis of simulations of polyethylene have identified two types of transition pairs that occur frequently, "gauche migration" and "kink creation/annihilation". Simulations of polybutadienes[25] and PEO[1] have shown that changes in chain structure allow additional types of correlated transitions. The possible impact of correlated motions on correlation function shape or the anisotropy of local dynamics has not been investigated. The fact that the pattern average angular displacements of Cartesian vectors associated with conformational transitions (eq 5 and Figure 4) does not change with the length of the time interval selected suggests that the impact of correlated transitions may be limited, but further investigation is warranted.

Further progress on these issues may require molecular dynamics simulations for a larger range of systems. Additional work is underway to extend these analyses to simulations of poly(oxymethylene), poly(tetramethylene oxide), and polyethylene solutions. Preliminary results for poly(tetramethylene oxide) solutions show that the simulations reproduce the trends in the relative anisotropies of the two types of methylene groups accurately.

Acknowledgment. The authors gratefully acknowledge many helpful conversations with Neil E. Moe. This work was supported in part by the National Institutes of Health (GM 46102-01; M.M.F) and the National Science Foundation (DMR-9424472; M.D.E.). The computers used in this work were also purchased through a grant from the NSF (CHE-9522057). M.M.F. also acknowledges the support of an R. C. Good Fellowship from Denison University.

References and Notes

(1) Fuson, M. M.; Ediger, M. D. *Macromolecules* **1997**, *30*, 5704.
(2) Weber, T. A.; Helfand, E. *J. Chem. Phys.* **1983**, *78*, 2881. Hall, C. K.; Helfand, E. *J. Chem. Phys.* **1982**, *77*, 3275.
(3) Takeuchi, H.; Roe, R.-J. *J. Chem. Phys.* **1991**, *94*, 7446.
(4) Adolf, D. B.; Ediger, M. D. *Macromolecules* **1991**, *24*, 5834. Ediger, M. D.; Adolf, D. B. *Macromolecules* **1992**, *25*, 1074.
(5) Smith, G. D.; Yoon, D. Y.; Jaffe, R. L. *Macromolecules* **1995**, *28*, 5897. Smith, G. D.; Yoon, D. Y.; Zhu, W.; Ediger, M. D. *Macromolecules* **1994**, *27*, 5563.
(6) Moe, N. E.; Ediger, M. D. *Macromolecules* **1995**, *28*, 2329.
(7) Moe, N. E.; Ediger, M. D. *Polymer* **1996**, *37*, 1787.
(8) Fuson, M. M.; Brown, M. S.; Grant, D. M.; Evans, G. T. *J. Am. Chem. Soc.* **1985**, *107*, 6695.
(9) Grant, D. M.; Mayne, C. L.; Liu, F.; Xiang, T.-X. *Chem. Rev.* **1991**, *91*, 1591.

(10) Werbelow, L. G.; Grant, D. M. *Adv. Magn. Reson.* **1977**, *9*, 189.
(11) Vold, R. L.; Vold, R. R. *Prog. Nucl. Magn. Reson. Spectrosc.* **1978**, *12*, 79.
(12) Canet, D. *Prog. Nucl. Magn. Reson. Spectrosc.* **1989**, *21*, 237.
(13) Werbelow, L. G.; Grant, D. M. *J. Chem. Phys.* **1975**, *63*, 4742.
(14) Fuson, M. M.; Anderson, D. J.; Liu, F.; Grant, D. M. *Macromolecules* **1991**, *24*, 2594.
(15) Fuson, M. M.; Miller, J. B. *Macromolecules* **1993**, *26*, 3218.
(16) Fuson, M. M.; Klei, B. R. *Macromolecules* **1996**, *29*, 5223.
(17) Depner, M.; Schurmann, B. L.; Auriemma, F. *Mol. Phys.* **1991**, *74*, 715.
(18) Schurmann, B. L. *Poly. Prepr. (Am. Chem. Soc., Div. Polym. Chem.)* **1992**, *33*, 568.
(19) Tasaki, K. *J. Am. Chem. Soc.* **1996**, *118*, 8459.
(20) Tasaki, K. *Macromolecules* **1996**, *29*, 8922.
(21) Smith, G. D.; Yoon, D. Y.; Jaffe, R. L.; Colby, R. H.; Krishnamoorti, R.; Fetters, L. J. *Macromolecules* **1995**, *28*, 5897.
(22) Smith, G. D.; Yoon, D. L.; Wade, C. G.; O'Leary, D.; Chen, A.; Jaffe, R. L. *J. Chem. Phys.* **1997**, *106*, 3798.
(23) Neyertz, S.; Brown, D. *J. Chem. Phys.* **1995**, *102*, 9725.
(24) Boyd, R. H.; Gee, R. H.; Han, J.; Jin, Y. *J. Chem. Phys.* **1994**, *101*, 788.
(25) Gee, R. H.; Boyd, R. H. *J. Chem. Phys.* **1994**, *101*, 8028.
(26) Kim, E.-G.; Mattice, W. L. *J. Chem. Phys.* **1994**, *101*, 6242.
(27) Bovee, W. M. M. J. *Mol. Phys.* **1975**, *29*, 1673.
(28) Liu, F.; Mayne, C. L.; Grant, D. M. *J. Magn. Reson.* **1989**, *84*, 344.
(29) Zheng, Z.; Mayne, C. L.; Grant, D. M. *J. Magn. Reson., Ser. A* **1993**, *103*, 268.
(30) Daragan, V. A.; Mayo, K. H. *Chem. Phys. Lett.* **1993**, *206*, 393.
(31) Khazanovich, T. N.; Zitserman, V. *Mol. Phys.* **1971**, *21*, 65.
(32) Rama Krishna, N.; Gordon, S. L. *J. Chem. Phys.* **1973**, *58*, 5687.
(33) Fuson, M. M.; Belu, A. M. *J. Magn. Reson., Ser. A* **1994**, *107*, 1.
(34) Alstrup, A. A. *Acta Chem. Scand.* **1979**, *A33*, 655.
(35) Bonham, R. A.; Bartell, L. S.; Kohl, D. A. *J. Am. Chem. Soc.* **1959**, *81*, 4765.
(36) Tasaki, K.; Abe, A. *Polym. J.* **1985**, *17*, 641.
(37) Liu, K.-J.; Ullman, R. *J. Chem. Phys.* **1968**, *48*, 1158.
(38) Breen, J.; van Duijin, D.; de Bleijser, J.; Leyte, J. C. *Ber. Bunsen-Ges Phys. Chem.* **1986**, *90*, 1112.
(39) Blieze, T. W. N.; van der Maarel, J. R. C.; Eisenbach, C. D.; Leyte, J. C. *Macromolecules* **1994**, *27*, 1355.
(40) Heatley, F.; Walton, I. *Polymer* **1976**, *17*, 1019.
(41) Williams, G.; Watts, D. C. *Trans. Faraday Soc.* **1970**, *66*, 80.
(42) Fuson, M. M.; Ediger, M. D. Unpublished results.
(43) Moe, N. E.; Ediger, M. D. *Macromolecules* **1996**, *29*, 5484.

MA970035S